A New Method for Six-Port Swept Frequency Automatic Network Analysis

LEOPOLDINE KALIOUBY AND RENATO G. BOSISIO, MEMBER, IEEE

Abstract —Six-port automatic network analyzers measure the reflection coefficient Γ by means of four power detectors. The amplitude and phase of Γ are then calculated using the values of the four power readings and the calibration constants at the frequency of measurement. This technique is generally used in a point-by-point measurement method. This paper presents a new method to obtain real-time swept frequency reflection coefficient measurements by using a six-port amplitude chart (SPAC) and a six-port phase chart (SPPC) plotted on a computer screen. The charts are precalculated for each frequency window, which manually (or automatically) scan the test band. Both six-port charts are plotted on the computer screen along with the analog signal from which is measured the modulus and phase of Γ within the frequency window. This method effectively allows frequency swept measurements of Γ across the test band. Such measurements are most important for the detection of spurious resonances or for fine circuit adjustments. Once the swept frequency tests of the microwave circuit are done, the usual six-port measurements may then be made at preselected frequency points with the assurance that no spurious response exists in between the frequency test points, and that circuit tuning has been optimized.

I. INTRODUCTION

SIX-PORT automatic network analyzers [1]–[3] measure the reflection coefficient Γ using four power measurements, P_3, P_4, P_5, and P_6, that can be expressed as follows:

$$P_3 = |aA + bB|^2 \quad (1)$$

$$P_4 = |aC + bD|^2 \quad (2)$$

$$P_5 = |aE + bF|^2 \quad (3)$$

$$P_6 = |aG + bH|^2 \quad (4)$$

where a and b are the reflected and incident waves ($\Gamma = a/b$, and $A, B, \cdots, H$ are complex constants of the six-port design.

For an ideal six-port $C = 0$, the ratios $-B/A$, $-F/E$, and H/G all have the same modulus that lies within the interval 0.5 and 1.5, and a phase difference of 120° [2]. The reflection coefficient Γ can be shown to be the intersection of three circles, with centers in the Γ plane, given by $-B/A$, $-D/C$, and $-H/G$ as shown in Fig. 1(a) and (b). For example, in this case, the intersection of circle C_1, of radius $\sqrt{P_3/P_4}$, with circle C_2 of radius $\sqrt{P_5/P_4}$, gives two possible solutions S_1 and S_2. Similarly, the intersection of circle C_1 with circle C_3, of radius $\sqrt{P_6/P_4}$, also gives two possible solutions S_1 and S_3. The reflection coefficient Γ is equal to the only solution common to both sets S_1.

In practice, a six-port is more easily realized [4] with standard components, such that $|B/A| = \sqrt{2}$, $|D/C| = |H/G| = 2$, with phase differences of 135°, 135°, and 90°.

Experimental measurements have shown that the six-port constants $A, B, \cdots, H$ diverge from design objectives and vary with frequency. Thus, precise evaluation of Γ requires a careful calibration at a given number of frequency points. For this reason, six-port measurements are normally done at predetermined discrete frequency points, and exclude continuous swept frequency measurements (CSFM). Swept frequency measurements are very useful in experimental development work, where it is often necessary to visualize the phase and amplitude of Γ, in real-time over a given bandwidth, say f_1 to f_2. So far, no method exists by which the six-port can be used in CSFM. This feature has been a major concern in the use of six-ports as automatic network analyzers (ANA) [4].

Engen has already referred to the possibility of using analog signals, corresponding to the power readings in order to display on an oscilloscope screen the modulus and phase of Γ, as a function of frequency [4]. However, the method requires the transmission of relatively weak analog signals, specific values of $A, B, \cdots, H$, and a constant incident power level; however, these conditions tend to reduce the usefulness of a six-port in a CSFM system.

In this paper, we derive a six-port amplitude chart (SPAC) to measure the modulus of Γ, and a six-port phase chart (SPPC) to measure the phase of Γ at either fixed frequencies or in a CSFM. Both charts may be separately plotted or superimposed on a computer screen along with an analog signal to indicate the phase and amplitude of Γ, over a given bandwidth, (f_1 to f_2).

The SPAC and SPPC charts may be derived by averaging the calibration measurements within a number of frequency intervals which, taken together, span the bandwidth of the six-port (typically 8:1). All of the calibration data is stored in the computer data bank for later use as required by the operating bandwidth (f_1–f_2). A single frequency sweep may also be made across the full test band at reduced accuracy by using an average SPAC and SPPC for the test band. The swept frequency interval f_1–f_2 is

Manuscript received April 17, 1984.
The authors are with the Ecóle Polytechnique, Electrical Engineering Department, Campus de l'Université de Montréal, P. O. Box 6079, Station "A", Montreal, Quebec, Canada H3C 3A7.

0018-9480/84/1200-1678$01.00 ©1984 IEEE

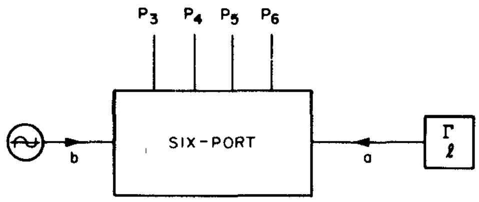

(a)

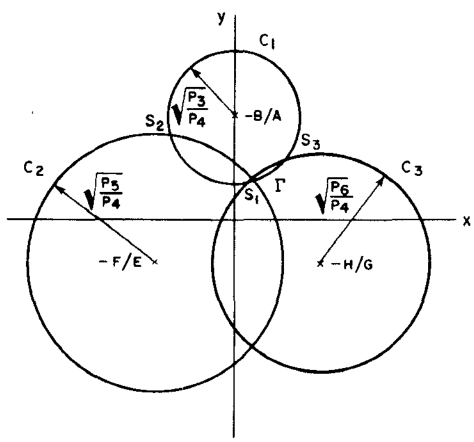

(b)

Fig. 1. (a) The six-port gives four output power readings. Each power level is a function of both the modulus and phase of the reflection coefficient Γ where $\Gamma = x + jy$. (b) Γ is calculated as the intersection of three circles in the Γ plane.

moved across the test band by varying the base frequency f, either manually or automatically across the desired frequency band. The scan rate is sufficiently slow to check for anonymous responses and to allow the computer to continuously refresh the SPAC and SPPC patterns on the screen as the value of f_1 changes.

II. Theory

For six-port automatic network analyzers, the power ratios P_3/P_4, P_5/P_4, and P_6/P_4 are given by, respectively, [2]:

$$\frac{P_3}{P_4} = \frac{|A\Gamma + B|^2}{|C\Gamma + D|} \tag{5}$$

$$\frac{P_5}{P_4} = \frac{|E\Gamma + F|^2}{|C\Gamma + D|} \tag{6}$$

$$\frac{P_6}{P_4} = \frac{|G\Gamma + H|^2}{|C\Gamma + D|}. \tag{7}$$

It's possible, using (5), (6), and (7), to calculate with calibrated values of $A, B, \cdots, H$, the loci of constant moduli and phase of Γ, as a function of P_3/P_4, P_5/P_4, and P_6/P_4. These charts are referred to as the six-port amplitude chart (SPAC) and the six-port phase chart (SPPC). The method of constructing these two charts is now given for the case of the symmetrical six-port junction.

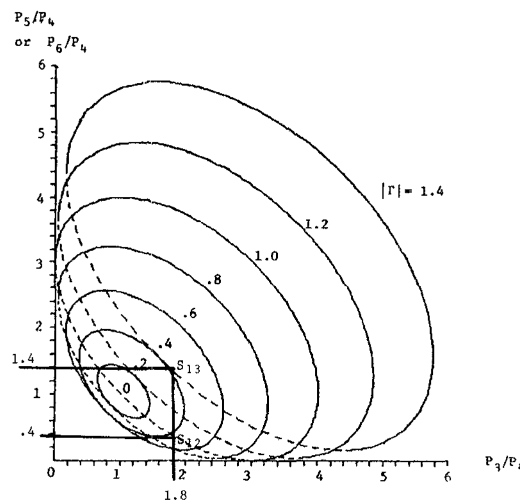

(a)

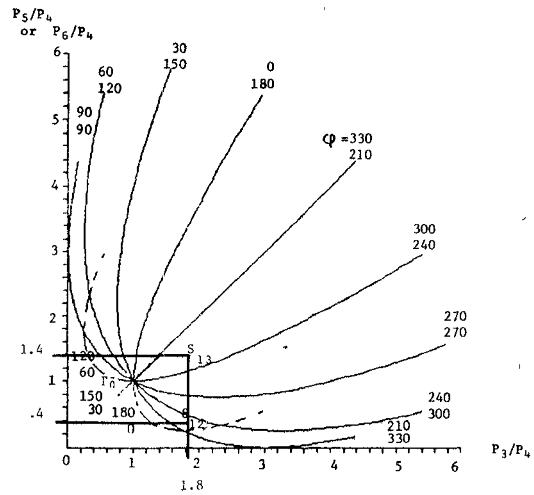

(b)

Fig. 2. (a) An SPAC showing locus of constant modulus of Γ, for a six-port assuming ideal 120° distribution. ——: the higher value of the two measurements of P_5/P_4 or P_6/P_4. ----: the lower value of the two measurements of P_5/P_4 or P_6/P_4. (b) An SPPC showing locus of constant phase (in degrees) of Γ, for a six-port assuming 120° distribution. ——: the higher value of the two measurements of P_5/P_4 or P_6/P_4. ----: the lower value of the two measurements of P_5/P_4 or P_6/P_4.

Ideal Six-Port with 120° Distribution

For this ideal six-port, we have

$$C = 0,\ |A|^2 = |D|^2 = |E|^2 = |G|^2$$
$$-B/A = 1\measuredangle 90°,\ -F/E = 1\measuredangle 210°, \text{and } -H/6 = 1\measuredangle 330°.$$

Equations (5), (6), and (7) can then be reduced to

$$P_3/P_4 = m^2 + m_3^2 - 2mm_3\cos(\varphi - \varphi_3) \tag{8}$$

$$P_5/P_4 = m^2 + m_5^2 - 2mm_5\cos(\varphi - \varphi_5) \tag{9}$$

$$P_6/P_4 = m^2 + m_6^2 - 2mm_6\cos(\varphi - \varphi_6) \tag{10}$$

where

$$\Gamma = m\measuredangle\varphi, \quad q_n = m_n\measuredangle\varphi_n, \qquad n = 3,5,6$$

with

$$q_3 = -B/A, \quad q_5 = -F/G, \quad q_6 = H/G$$

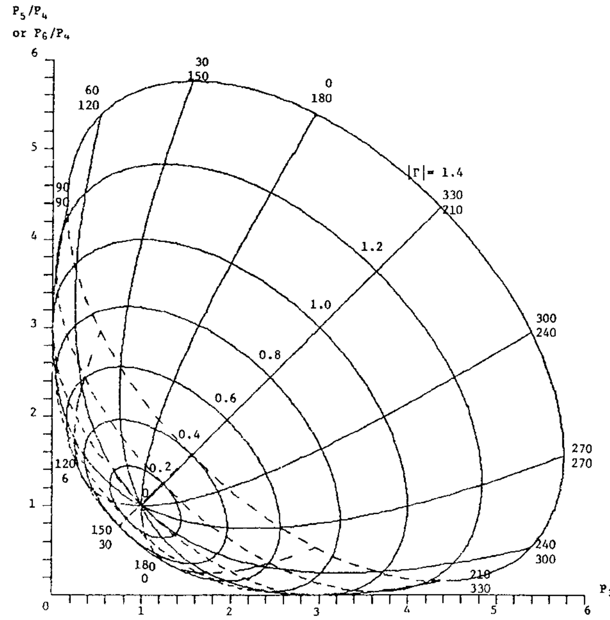

Fig. 3. Superimposed SPAC and SPPC showing locus of constant modulus and phase (in degrees) of Γ, for a six-port assuming ideal 120° distribution. Measurements were made with system shown in Fig. 5.

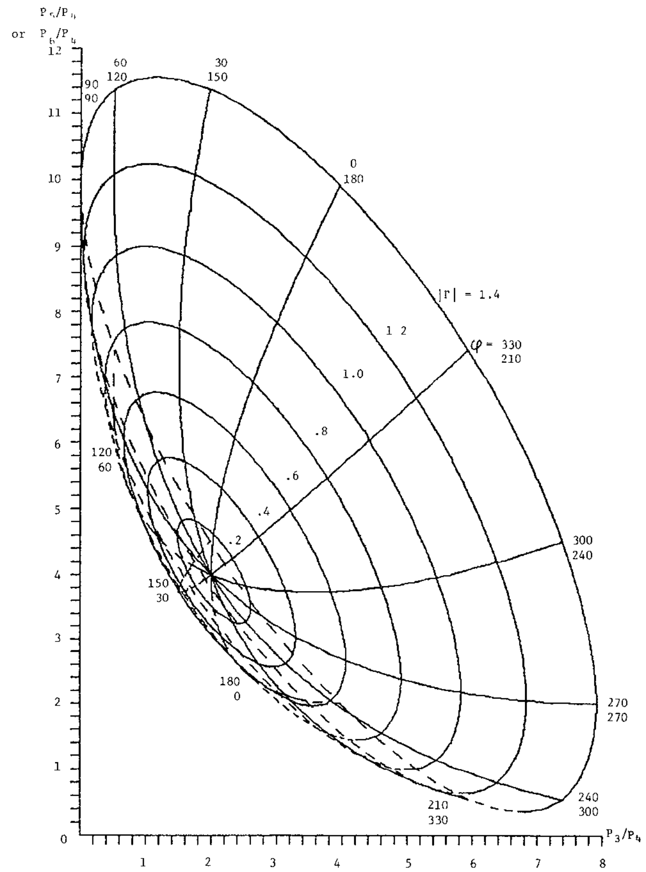

Fig. 4. Superimposed SPAC and SPPC for a six-port assuming 135–135–90° distribution.

where m is the modulus and φ the phase of Γ, and m_n is the modulus and φ_n the phase of q_n. The loci of constant moduli and phase of Γ are calculated by using (8), (9), and (10). The results are shown in Fig. 2(a) and (b). The loci of the constant moduli are obtained by letting m take the values of $0, 0.2, 0.4, \cdots, 1, 4$, and by letting φ vary between 0° and 360°. Similarly, the loci of the constant phases are obtained by letting φ take, successively, the values of $0, 30, 60, \cdots, 360°$ and letting m vary between 0 and 1.4.

Let's first explain some of the results obtained for the six-port amplitude chart (SPAC) in Fig. 2(a). It's seen that the loci of constant moduli of Γ form a set of closed curves, with increasing dimensions as the modulus of Γ increases. For every pair of power ratios P_3/P_4 and P_5/P_4 (or P_6/P_4), there always exists two possible solutions, one shown by solid lines, the other by dashed lines. These two solutions correspond to the two possible intersections of circle of radius $\sqrt{P_3/P_4}$ and circle of radius $\sqrt{P_5/P_4}$ (or $\sqrt{P_6/P_4}$) in the Γ plane. For example, if $P_3/P_4 = 1.8$ and $P_5/P_4 = 0.4$, then $|\Gamma| = 0.4$ or 1.0 (pt S_{12}), corresponding to solutions S_1 or S_2. Similarly, if $P_3/P_4 = 1.8$ and $P_6/P_4 = 1.4$, then $|\Gamma| = 0.4$ or 1.4 (pt S_{13}, corresponding to solutions S_1 or S_3). The modulus of the reflection coefficient Γ is then the only solution common to both sets, which is S_1, $|\Gamma| = 0.4$. Note that, if only the maximum value of P_5/P_4 and P_6/P_4 is considered, then $|\Gamma|$ is the only solution shown in solid lines, which is 0.4.

Let's now examine the six-port phase chart (SPPC) (Fig. 2(b). It's seen that the loci of constant phases form a set of open curves, all passing by the point Γ_0 corresponding to $|\Gamma| = 0$. To each curve, two phases are associated, one for P_5/P_4 and the other for P_6/P_4. The number at the top of the set of two phase numbers, identifying each curve in Fig. 2(b), corresponds to the P_5/P_4 measurement. The phase number situated in the bottom position corresponds to the P_6/P_4 measurements. Using the same numerical example, it's seen that, if $P_3/P_4 = 1.8$ and $P_5/P_4 = 0.4$, $\varphi = 225$ or 5 (pt S_{12}). Similarly, if $P_3/P_4 = 1.8$, and $P_6/P_4 = 1.4$, $\varphi = 225$ or 25 (pt S_{13}). Thus, the phase φ is the only solution common to both sets, which is $\varphi = 225$. Also, if only the maximum value of P_5/P_4 or P_6/P_4 is considered, φ is the solution in solid lines. In this example, it's $\varphi = 225$. A plot of the analog signals P_3/P_4 in the x axis, and P_5/P_4 or P_6/P_4 in the y axis as the frequency is swept inside a given frequency window provides a measurement of both the modulus ($|\Gamma|$) and phase (φ) of Γ from the calibrated SPAC and SPPC. Fig. 3 shows both SPAC and SPPC on the same screen for the case discussed above.

Fig. 4 shows similar results obtained with a six-port design in which the angle separating the centers of the power circles are 135°, 135°, and 90°; that is, with $q_3 = \sqrt{2}\measuredangle 90$, $q_5 = 2\measuredangle 225$, and $q_6 = 2\measuredangle 315$.

III. Experimental Equipment

For the first experiments, an existing six-port ANA system (Fig. 5), was used to plot on a SPAC and SPPC point-by-point measurement results obtained with a sliding short and a matched load for an existing symmetrical six-port, (see (3)). Fig. 6 shows a proposed system under development for use with an HP9816 computer.

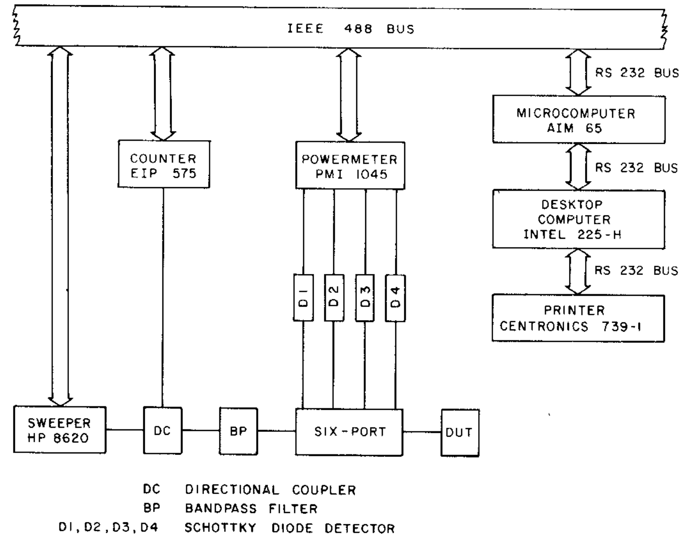

Fig. 5. Experimental system used for experimental measurements at single frequency points made with an Intel computer.

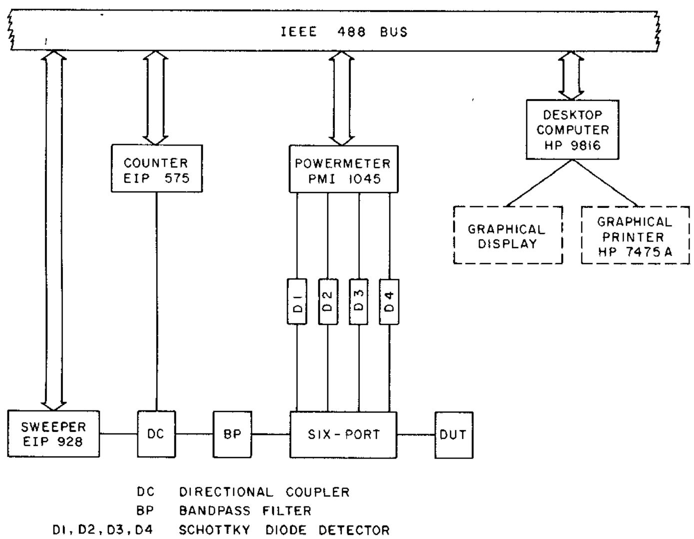

Fig. 6. System for continuous swept frequency testing and single frequency point testing using an HP9816 computer.

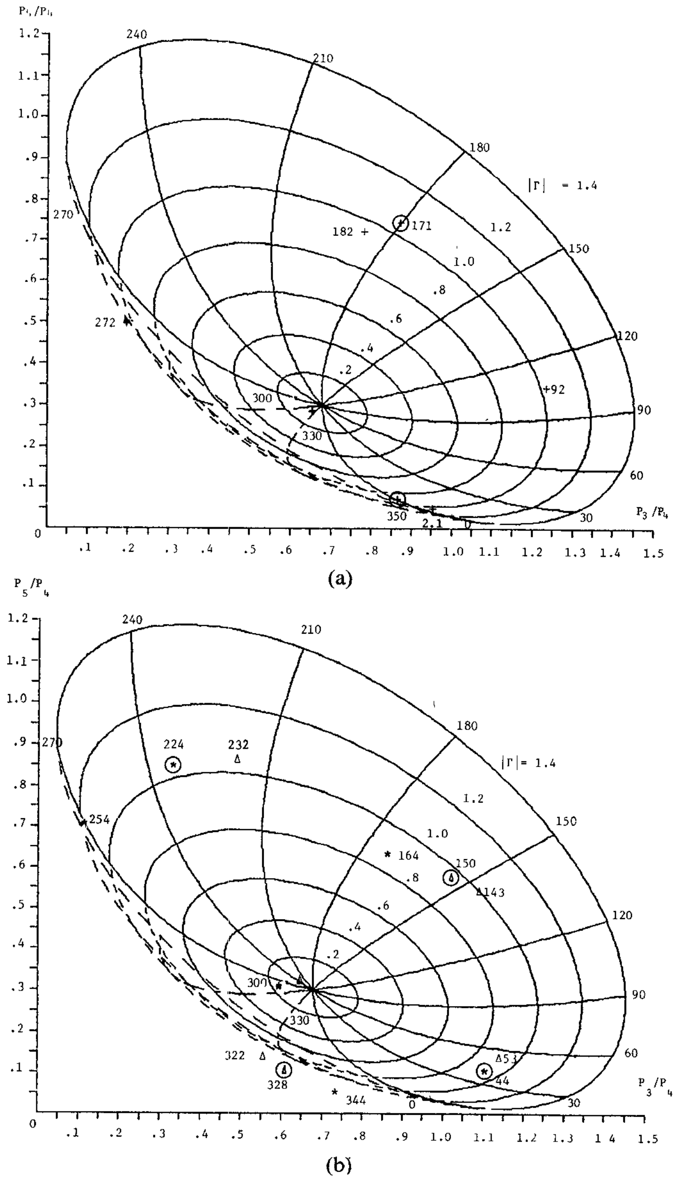

Fig. 7. (a) An SPAC and SPPC chart at 3 GHz (+) obtained with values of $A, B, \cdots, H$ as measured from an actual 120° six-port. Encircled data points near $|\Gamma| = 1$ correspond to fixed short, and open short and the noncircled data points correspond to a sliding short. For the test data near $|\Gamma| = 0$, the experimental point corresponds to a matched-load condition. Measurements made with system shown in Fig. 5. (b) Same measurements repeated at 2.9 GHz (*) and 3.1 GHz (Δ) using calibration data taken at 3.0 GHz. An offset phase has been taken into account ($\varphi_{off} = 52°$ at 2.9 GHz and 21° at 3.1 GHz).

IV. Experimental Results and Discussion

The ideal 120° six-port, designed in our laboratory [3] using microwave integrated technology has been characterized in the interval 2–4 GHz, with the experimental set up shown in Figs. 5 and 6. Measurements taken with the system in Fig. 5 for P_3/P_4 and P_5/P_4, at 3 GHz is given in Fig. 7(a), in the case of a sliding short, fixed short, open short, and matched load conditions. Fig. 7(b) shows similar test results obtained at 2.9 and 3.1 GHz. The SPAC and SPPC, shown in Fig. 7(a) and (b), were obtained from calibration data taken at one frequency only (3.0 GHz). The calibration data is as follows:

$$|A/C|^2 = 8.22, \quad |E/C|^2 = 3.40, \quad |G/C| = 5.21$$
$$-D/C = 6.06\measuredangle 3°, \quad -B/A = 1.74\measuredangle 3,$$
$$-F/E = 1.80\measuredangle 265, \quad -H/G = 1.43\measuredangle 90.$$

As expected, the error is smaller when the test frequency is equal to the calibration frequency (Fig. 7(a)). In this case, the measurement error is less than 5 percent in amplitude and less than 10° in phase. However, at 2.9 and 3.1 GHz (Fig. 7(b)), the data points for short circuit, fixed short, open short, matchled load, and sliding short produce the following errors: $\Delta\,|\Gamma| < 10°$ and $\Delta\varphi < 12°$. In both cases, the offset phase φ_{off} is taken into account (this value is displayed in the computer). Absolute errors in CSFM are not important in the detection of spurious responses or for optimizing circuit performance by tuning procedures. The above measurement errors may be reduced if necessary by

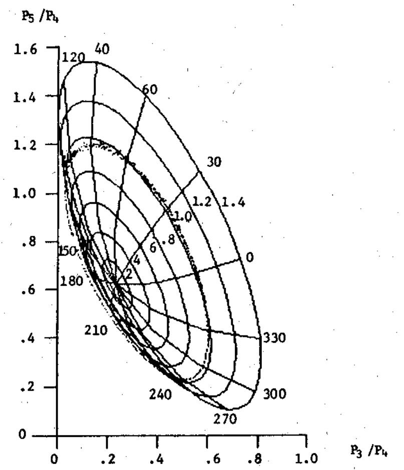

Fig. 8. An SPAC and an SPPC chart at 3 GHz with values of A, $B,\cdots,H$ as measured from a second 120° six-port construction. The dotted line, close to $|\Gamma|=1$ contour line, was obtained by moving a sliding short through 360° at an operating frequency of 3.0 GHz using the measurement system shown in Fig. 6.

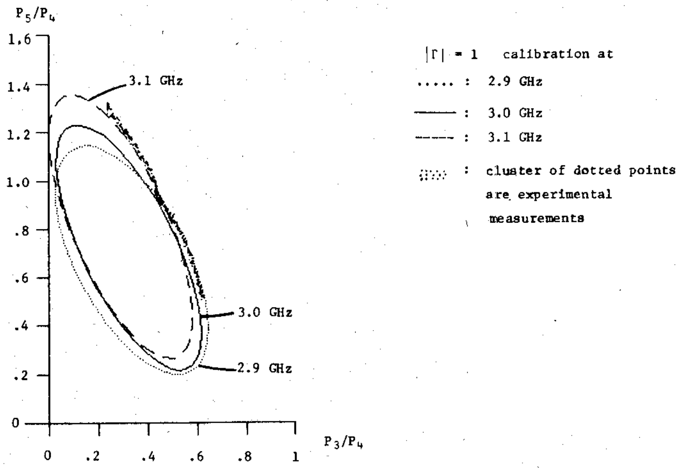

Fig. 9. SPAC contours for $|\Gamma|=1$ obtained from calibration data taken at 2.9, 3.0, and 3.1 GHz. (The SPPC information is not shown and is best displayed with a color screen). The line formed by the clustered points was obtained experimentally by varying the signal frequency from 2.9 to 3.1 GHz with a fixed short on the six-port output terminal. Measurements were made with the measurement system shown in Fig. 6.

using an average SPAC and SPPC within a reduced frequency interval (i.e., less than 200 MHz).

Fig. 8 shows an SPAC and a SPPC obtained with the measurement system in Fig. 6 using a second six-port of similar design to the one reported above. In this case, the calibration data at 3.0 GHz is as follows:

$$|A/C|^2=138.0, \quad |E/C|^2=104.9, \quad |G/C|^2=112.9$$
$$-D/C=36.74\measuredangle 100, \quad -B/A=1.52\measuredangle 127,$$
$$-F/4=3.0\measuredangle 262, \quad -H/G=1.36\measuredangle 20.$$

It is seen that the measured values of $|\Gamma|$ for a sliding short are close to the $|\Gamma|=1$ contour, as expected. The phase change around the $|\Gamma|=1$ contour corresponds to a displacement of one wavelength for the sliding short position.

Fig. 9 shows the measured reflection coefficient for a fixed short position when the frequency is varied from 2.9 to 3.1 GHz. The three loci for $|\Gamma|=1$, as obtained from the calibration data, taken at the three frequency points is also shown on the computer screen. It is seen that the SPAC and SPPC must be refreshed when manually scanning f_1 across a large test band using an electronically swept frequency interval—f_2-f_1. Using present day computers, it is possible to store a large number of SPAC and SPPC and present these on the computer screen as required by the test frequency band.

V. Conclusion

A six-port amplitude chart (SPAC) and a six-port phase chart (SPPC) displayed on a computer screen can be used with sufficiently good accuracy in CSFM measurements for the detection of spurious responses and for tuning microwave circuits. The accuracy of the phase (10 percent) and amplitude (10 percent) measurements obtained for a 200-MHz interval (f_2-f_1) can be improved by reducing the swept frequency interval (f_2-f_1). Circuits may be tested, for spurious responses and tuning purposes, by manually scanning the f_2-f_1 window across the test band while the SPAC and SPPC are refreshed as required by the test frequency. The same six-port measurement system equipment is then used at single frequency points to obtain the usual high precision [3] of six-port measurements ($\Delta|\Gamma| < 0.01$ and $\Delta\varphi < 4°$).

References

[1] G. F. Engen and C. A. Hoer, "Applications of an arbitrary six-port junction to power measurement problems," *IEEE Trans. Instrum. Meas.*, vol. IM-21, no. 4, pp. 470–474, Dec. 1972.

[2] G. F. Engen, "The six-port reflectometer: An alternative network analyzer," *IEEE Trans. Microwave Theory Tech.*, vol. MTT-25, pp. 1075–1079, Dec. 1977.

[3] S. H. Li, "Automatic Analysis of Multi-Port Microwave Network," Ph.D. dissertation, Ecole Polytechnique de Montreal, 1982.

[4] G. F. Engen, "An improved circuit for implementing the six-port technique of microwave instruments," *IEEE Trans. Microwave Theory Tech.*, vol. MTT-25, pp. 1080–1083, Dec. 1977.

[5] G. F. Engen, "Calibrating the six-port reflectometer by means of sliding terminations," *IEEE Trans. Instrum. Meas.*, vol. IM-22, no. 4, pp. 295–299, Dec. 1973.

[6] G. P. Riblet, "A compact waveguide 'resolver' for the accurate measurement of complex reflection and transmission coefficient using the six-port measurement concept," *IEEE Trans. Microwave Theory Tech.*, vol. MTT-29, pp. 115–162, Feb. 1982.

[7] S. H. Li and R. G. Bosisio, "Measurement of complex reflection coefficient by means of a five-port reflectometer," *IEEE Trans. Microwave Theory Tech.*, vol. MTT-31, pp. 321–326, Apr. 1983.